Journal of Alloys and Compounds 509 (2011) 8683–8687

Contents lists available at ScienceDirect

Journal of Alloys and Compounds

journal homepage: www.elsevier.com/locate/jallcom

Role of BaO/SrO layers in deciding the electronic structure of $Cu_{0.3}Co_{0.7}Ba_{2-x}Sr_xYCu_2O_{7+\delta}$ (CoCu-1212) $x = 0$, 1 and 2

Shiva Kumar Singh [a,b,*], M. Husain [b], H. Kishan [a], V.P.S. Awana [a]

[a] National Physical Laboratory (CSIR), New Delhi 110012, India
[b] Department of Physics, Jamia Millia Islamia, New Delhi 110025, India

ARTICLE INFO

Article history:
Received 10 March 2011
Received in revised form 22 May 2011
Accepted 28 May 2011
Available online 21 June 2011

Keywords:
Structural refinement
Tolerance factor
XPS
Valence state
Resistivity
Magnetization

ABSTRACT

In this paper we report the change in electronic structure of $Cu_{0.3}Co_{0.7}Ba_{2-x}Sr_xYCu_2O_{7+\delta}$ with change in structural pressure. Rietveld refined X-ray diffraction (XRD) pattern shows that the samples are phase pure. Decrease in lattice parameters with increasing x, confirms replacement by Sr ion at Ba ion site. The calculated tolerance factor of the systems is in accord with lattice parameter changes. The X-ray photoelectron spectroscopy (XPS) is made to find out the variation in ionic state of Co and Cu with ionic size variation in BaO/SrO layers. Effect of the same on the electronic structure and transport properties is explored. The XPS measurement reveals that Cu is in mixed 1+/2+ state and variation in valence state is non-monotonous with increasing x. Whereas Co is in mixed 3+/4+ state and with increasing x its valence state is increasing. The observed changes in electronic structure are subject of structural changes. The resistivity measurement shows that normal state conductivity decreases with increasing x. Resistivity behaviour indicates about holes in Cu/CoO_x planes taking part in charge transport. The magnetic measurement (M–T and M–H) shows that paramagnetic nature for all the compositions. The presence of Cu ions in Cu/CoO_x chains/planes results in paramagnetic behaviour.

1. Introduction

The structure of $YBa_2Cu_3O_{7-\delta}$ ($CuBa_2YCu_2O_{7-\delta}$, Cu-1212) or M-1212 (Cu replaced with other metal elements in CuO_x chains) structure can be viewed as (Ba, Sr)O/CuO_2/RE/CuO_2/(Ba, Sr)O slabs are interconnected through a sheet of M and O with variable composition of MO_x. Charge transport and high temperature superconductivity (HTSC) is believed to reside in the CuO_2 planes of all known HTSC cuprates, except that CuO_x chains have been reported to participate in the b-axis transport of Cu-1212 [1]. In Cu-1212 there are two different Cu sites, namely Cu1 and Cu2. Cu1 resides in CuO_x chains and Cu2 in superconducting CuO_2 planes. It is believed that BaO/SrO layers work as spacers and play a significant role in structure formation and in its stability [2,3]. It is also believed that superconductivity can possibly be introduced in non-superconducting samples or transition temperature (T_c) can be enhanced (changed) in superconducting samples by creating structural pressure, i.e. replacing some element with an element having smaller radii. Optimal plane charge order in superconducting cuprates is studied in [4]. It is concluded that superconductivity is a charge order related phenomenon and can be manipulated by lattice pressure. Ionic size variation at rare-earth (RE) site is reported in Ref. [5]. $REBa_2Cu_{3-x}Zn_xO_{7-\delta}$ compositions with various rare earth elements are studied. With increasing ionic radii T_c decreases along with increase in normal state resistivity. It was found that the superconducting transition width ΔT_c, increases with increasing Zn concentration for each RE, and also with increasing ionic radius of the rare-earth element when the Zn concentration is kept constant.

We here replaced larger Ba (1.35 Å) atoms in the unit cell with smaller Sr (1.18 Å) atoms [6]. The properties of Sr doped Y-124 at Ba site have been studied and decrease in Cu1–Cu2 bond distances was observed while T_c remained constant [7]. Generally the crystal structure of cuprates is subject of, atoms and stoichiometry of oxygen in MO_x chains/planes [8–13]. But the Ba/SrO layers also play a key role in deciding the crystal structure of the cuprates as well as in structure stability. The $YBa_2Cu_3O_{7-\delta}$ compound crystallizes in orthorhombic $Pmmm$ space group whereas $YSr_2Cu_3O_{7-\delta}$ structure does not crystallize at normal pressure. This is due to smaller ionic radii of Sr in comparison to Ba. It is reported, that Co-1212 ($CoSr_2YCu_2O_{7+\delta}$) phase has orthorhombic $Ima2$ space group structure with CoO_4 tetrahedra in MO_x chain/planes. It is due to rotation of CoO_4 tetrahedra in two directions in the consecutive unit cell [11–13], forming two different chains left handed oriented (L-chains) and right handed oriented (R-chains). Order-

* Corresponding author at: National Physical Laboratory (CSIR), New Delhi 110012, India. Tel.: +91 11 45609210; fax: +91 11 45609310.
E-mail addresses: singhsk@mail.nplindia.ernet.in (S.K. Singh), awana@mail.nplindia.ernet.in (V.P.S. Awana).
URL: http://www.freewebs.com/vpsawana/ (V.P.S. Awana).

0925-8388/$ – see front matter © 2011 Elsevier B.V. All rights reserved.
doi:10.1016/j.jallcom.2011.05.109

ing of the two types of chains presumably occurs so that the total lattice energy would be reduced. In crystallization of *Ima2* space group the unit cell gets doubled than that of *P4/mmm* space group. This also causes the increase of *b* and *c* parameters by $\sqrt{2}$ times [13]. However, the Co-1212 phase with Ba ion on Sr ion site ($Cu_{1-x}Co_xBa_2YCu_2O_{7+\delta}$, $x = 0.84$ composition) was reported to crystallize in tetragonal *P4/mmm* space group [14]. In contrast to some metal elements such as Fe, replaces Cu in CuO_2 planes along with CuO_x chains [8], Co generally replaces Cu1 in CuO_x chains. It had been observed that Co-doping at Cu2 sites somehow localizes the carriers at Co sites and decreases the density of mobile carriers in the superconducting CuO_2 planes [15]. However, thermogravimetric and neutron diffraction studies of metal substituted $YBa_2Cu_{3-x}M_xO_{7-\delta}$ [16] perovskites show evidence of major substitution of Co atoms at CuO_x chain sites.

Electronic structure studies such as X-ray and ultraviolet photoelectron spectroscopy (XPS and UPS) and resonant photoemission have, thus far, been widely acceptable for Cu-1212 [17,18]. These studies have established the nominal presence of the Cu^{3+} oxidation state which is important for some theories. XPS measurements had been made to calculate the oxidation state of copper and oxygen in Cu-1212 [17] below and above T_c. They found that formation of Cu^{1+} below T_c due to dimerization of oxygen and concomitant reduction of Cu^{2+}. The temperature dependent XPS study reveals that increase of CuO spectra FWHM in superconducting state [19]. They observed presence of Cu^{3+} and Cu^{2+} at low temperature in superconducting samples. Here, by XPS study we have found out the ionic state of Co and Cu in $Cu_{0.3}Co_{0.7}Ba_{2-x}Sr_xYCu_2O_{7+\delta}$ ($0.0 \le x \le 2.0$). The change in ionic state is studied with ionic size variation in spacer layers of cuprates. Its impact on transport properties is also studied. The particular composition ($Cu_{0.3}Co_{0.7}$) is taken due to, in case of $x = 2$ structure does not form with lower concentration of Co (<40%) at atmospheric pressure whereas in case of $x = 0$ extra phases appear with concentration of Co > 70%. Observed change in ionic state is correlated with ionic size and structural changes in unit cell.

2. Experimental

The samples are synthesized in air by solid-state reaction route. The stoichiometric mixture of Co_3O_4, $BaCO_3$, $SrCO_3$, Y_2O_3, and CuO are ground thoroughly, calcined at 900 °C for 12 h and then pre-sintered at 920 °C and 940 °C for 20 h with intermediate grindings. Finally, the powders are palletized and sintered at 940 °C for 20 h in air. The phase formation is checked for each sample with powder diffractometer, Rigaku (Cu Kα radiation) at room temperature. The phase purity analysis and lattice parameter refining are performed by Rietveld refinement programme (Fullprof version). The samples have been characterized by X-ray photoelectron spectroscopy, working at a base pressure of 5×10^{-10} Torr. The chamber is equipped with a dual anode Mg Kα (1253.6 eV) and Al Kα (1486.6 eV) X-ray sources and a high-resolution hemispherical electron energy analyzer. We have used Mg Kα X-ray source for our analysis. The calibration of the binding energy scale has been done with the C (1s) line at 284.6 eV. The core level spectra of Co and Cu have been deconvoluted in to the Gaussian components. The resistivity measurements of all samples are measured with standard four-probe method using APD cryogenics-HC2 Closed Cycle Refrigerator. The magnetization measurements are carried out applying a field magnitude up to 1 T using Physical Properties Measurement system-Quantum Designed PPMS-14T.

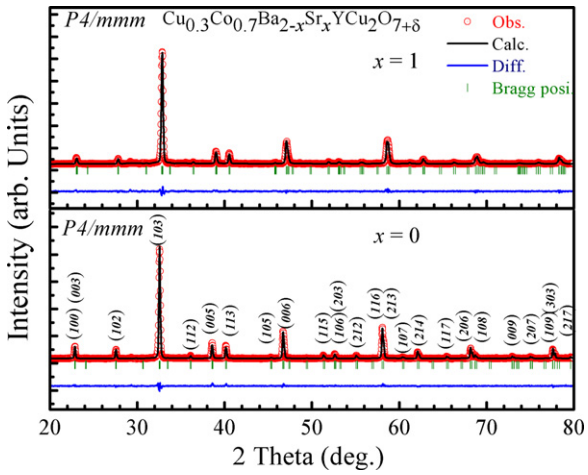

Fig. 1. Rietveld fitted XRD pattern of $Cu_{0.3}Co_{0.7}Ba_{2-x}Sr_xYCu_2O_{7+\delta}$ ($x = 0$ and 1) with space group *P4/mmm*.

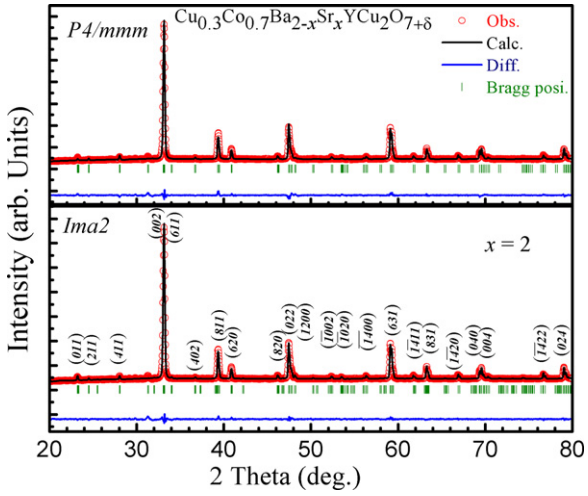

Fig. 2. Rietveld fitted XRD pattern of $Cu_{0.3}Co_{0.7}Ba_{2-x}Sr_xYCu_2O_{7+\delta}$ ($x = 2$) sample with space group *P4/mmm* and *Ima2*.

3. Results and discussion

All the samples are crystallized in single phase. This is confirmed from the Rietveld analysis of powder X-ray diffraction pattern. All the compositions ($x = 0$, 1 and 2) are fitted in tetragonal *P4/mmm* space group (Figs. 1 and 2). The monotonic decrease in lattice parameter clearly indicates that Sr^{2+} ion with smaller ionic radii (1.18 Å *CN VI*) replacing Ba^{2+} with larger ionic radii (1.35 Å *CN VI*) (Table 1). The same can be observed in XRD pattern, as there is shift in (1 0 3) peak towards higher angle side (Fig. 3). However, the $x = 2$ sample ($Cu_{0.30}Co_{0.70}Sr_2YCu_2O_{7+\delta}$) shows good fit in orthorhombic

Table 1
Rietveld refined lattice parameters, unit cell volume and calculated tolerance factor of $Cu_{0.3}Co_{0.7}Ba_{2-x}Sr_xYCu_2O_{7+\delta}$ ($x = 0$, 1 and 2).

$Cu_{0.3}Co_{0.7}Ba_{2-x}Sr_xYCu_2O_7$	$x = 0$	$x = 1$	$x = 2$ *P4/mmm*	$x = 2$ *Ima2*
a (Å)	3.886 (7)	3.858 (2)	3.828 (3)	22.840 (2)
b (Å)	3.886 (7)	3.858 (2)	3.828 (3)	5.416 (1)
c (Å)	11.663 (7)	11.523 (6)	11.420 (2)	5.412 (9)
V (Å^3)	176.199 (9)	171.514 (9)	167.379 (6)	669.618(4)
Co-O1 bond length (Å)	1.943 (3)	1.929 (1)	1.914 (1)	1.667 (5)
Chi^2	2.43	2.96	2.85	2.07
r_p	3.71	3.22	2.37	2.07
r_p	4.34	4.13	3.33	2.84
Tolerance factor '*t*'	0.8835	0.8644	0.8453	

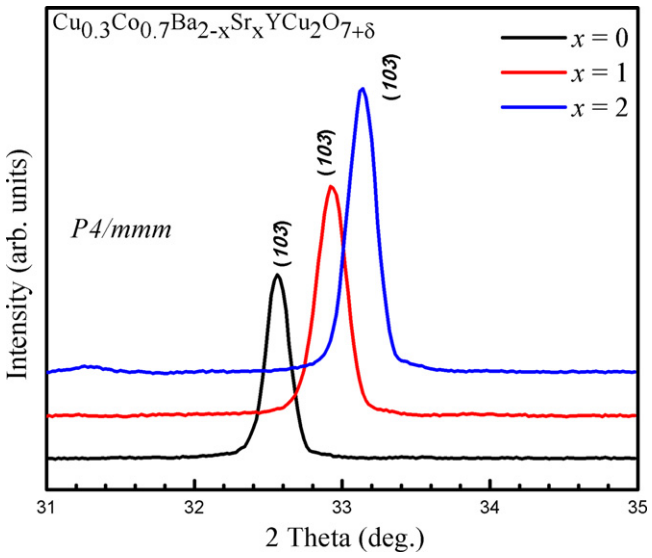

Fig. 3. X-ray pattern of main 1 0 3 peak of *P4/mmm* space group. It shows shift towards higher angle in 2θ as volume decreases in $(0 \le x \le 2)$ in *P4/mmm* space group.

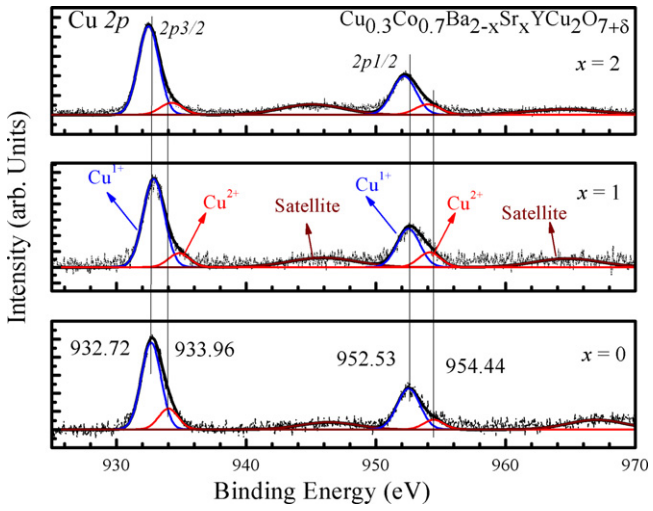

Fig. 4. The Cu (2p) XPS spectra of the $Cu_{0.3}Co_{0.7}Ba_{2-x}Sr_xYCu_2O_{7+\delta}$ ($x = 0$, 1 and 2). The dashed line represents the experimental curve and the solid line represents the resultant of fitted curve of various $Cu^{1+/2+}$ components.

Ima2 space group also (Fig. 2). The fitting parameters indicate that it is nearer to orthorhombic structure than tetragonal (Table 1). The stability of the pervoskite structure can be tested by geometrical parameter named tolerance factor '*t*'. For a pervoskite ABO_3 the tolerance factor is defined as: $t = (r_A + r_O)/2^{1/2}(r_B + r_O)$ [20] where r_A, r_O and r_B are ionic radii of A, O and B ions, respectively. The pervoskite structure can be formed for $0.8 < t < 1.0$. Since the Cu1212 (Y123) structure is a distorted layer pervoskite structure, the tolerance factor should still be valid to describe the stability of this. In the sense of average structural view the tolerance factor of our samples can be calculated as:

$$t = (1/3r_Y + 2/3r_{Ba,Sr} + r_O)/2^{1/2}(r_{CuCo} + r_O)$$

The tolerance factor calculated for all the compositions is shown in Table 1. Calculation of the tolerance factor is done considering the valence state and ionic radii as: Y^{3+} (1.019 Å), Ba^{2+} (1.35 Å), Sr^{2+} (1.18 Å), Cu^{1+} (0.77 Å), Co^{3+} (0.545 Å) and O^{2-} (1.38 Å) [6]. There is a decrease in tolerance factor of around 4% which is in accord with decrease of lattice parameters. It is considered that decrease in lattice parameters should cause increase in electronic pressure which may result in increase of holes in CuO_2 planes. This should result in increase of Cu valence state. But our findings are different than this.

To find out the oxidation states of Cu and Co the XPS study has been carried out. The Cu (2p) and Co (2p) core level spectra have been deconvoluted in to the different Gaussian component to find out the contribution of different ionic states. The deconvoluted Cu (2p) core level spectra for all samples are shown in Fig. 4. Cu ($2p_{3/2}$ and $2p_{1/2}$) core level spectra is deconvoluted in peaks at the binding energy of 932.72 eV and 933.96 eV for Cu ($2p_{3/2}$) and 952.53 eV and 954.44 eV for Cu ($2p_{1/2}$) in all compositions (Fig. 4). Satellite peaks are also associated with the main peaks at binding energy 945.40 eV for Cu ($2p_{3/2}$) and 964.54 eV for Cu ($2p_{1/2}$). Comparison of studied samples binding energy with earlier reported literature shows that presence of Cu in Cu^{1+} {932.72 eV for Cu ($2p_{3/2}$) and 952.53 eV for Cu ($2p_{1/2}$)} and Cu^{2+} {933.96 eV for Cu ($2p_{3/2}$) and 954.44 eV for Cu ($2p_{1/2}$)} [17,21–23]. The binding energy of Cu^{2+} component is slightly greater than earlier reported values [17,19,21–23]. The curve shows the domination of Cu^{1+} state over Cu^{2+} state in all compositions. However, temperature dependent (300 K, 80 K) XPS study made for superconducting Y-123 (Cu-1212) sample shows that majority of the oxidation state of Cu atoms, is Cu^{2+} at both temperatures [19]. Also, in superconducting state it shows some broadening in FWHM of the spectra. Major presence of Cu atoms in Cu^{1+} state could be the reason behind absence of superconductivity in studied samples. In the comparison of the spectrum of $x = 0$, the binding energy of two main component of Cu ($2p_{3/2}$ and $2p_{1/2}$), the spectrum of the sample $x = 1$, shifts towards higher binding energy. But there is decrease in valence state of Cu ion in $x = 2$ sample. The deconvoluted Co (2p) core level spectra for all samples are shown in Fig. 5. In the spectrum of Co, the binding energy of two main component of Co ($2p_{3/2}$ and $2p_{1/2}$) in samples $x = 1$ and 2, shifts towards higher binding energy than that in the spectrum of $x = 0$. Peak broadening is also observed in $x = 2$ composition in comparison to $x = 0$. Deconvolution of Co (2p) core level spectra shows the presence of Co^{3+} and Co^{4+} with a satellite peak, at the binding energy of 779.50 eV and 781.20 eV for Co ($2p_{3/2}$) and 794.81 eV and 796.61 eV for Co ($2p_{1/2}$), respectively in all compositions. The similar kinds of results have also been reported in literature regarding concentration and binding energy of $Co^{3+/4+}$ [24–26]. Curve shows the domination of Co^{3+} state over Co^{4+} state for $x = 0$ and 1 sample, but for $x = 2$ both states are almost equal.

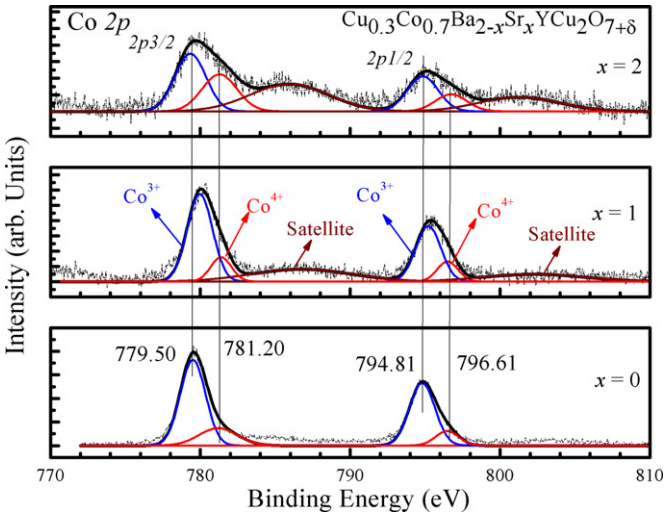

Fig. 5. The Co (2p) XPS spectra of the $Cu_{0.3}Co_{0.7}Ba_{2-x}Sr_xYCu_2O_{7+\delta}$ ($x = 0$, 1 and 2). The dashed line represents the experimental curve and the solid line represents the resultant of fitted curve of various $Co^{3+/4+}$ components.

The Cu ion valence state variation is non-monotonous, whereas the valence state of Co is increasing monotonically. The observed behaviour can be explained as; in $x = 1$ the small increase in valance of Cu is due to the chemical pressure (smaller Sr ions). In $x = 2$ the decrease in valance state of Cu may be due to structural changes. Since $CoSr_2YCu_2O_{7+\delta}$ is crystallize in orthorhombic *Ima2* [8,11–13,24]. Our $x = 2$ sample has 30% Cu at Co site hence it is more probable that it would be crystallized in orthorhombic *Ima2* space group. For further confirmation we fitted it in orthorhombic *Ima2* space group and it shows a good fit. However, it is closer to orthorhombic phase than tetragonal phase since fitting parameters are better for orthorhombic phase (Table 1). The CoO_6 octahedra of *P4/mmm* space group converts in CoO_4 tetrahedra of *Ima2* space group. The tendency of CoO_4 tetrahedra rotation in different direction in consecutive unit cells leads to formation of chains oriented in Left handed (L-chains) and Right handed (R-chains). An appreciable increase in Co valence state of $x = 2$ composition may be due to presence of these chains. The high resolution electron microscopy (HREM) study made by Nagai et al. [13] suggests that the intralayer interaction between the chains is strong because of shortness of the distance between them. This is the reason for the general phenomenon of intralayer ordering of the two types of chains. The shortness of distances between the chains may cause increase of effective oxygen coordination with Co-atoms which ultimately results in increased valence state of Co ions. It can be seen that calculated Co-O1 (O1 is the oxygen atom in Cu/CoO_x chains/planes) bond length is indeed getting shortened with increasing x and least for $x = 2$ composition in *Ima2* space group. Bond lengths, calculated through Rietveld analysis are given in Table 1. This shortening in bond length is thus, causing increase in valence state of Co ions. Increase in Co valence state may lead to decrease of effective Cu valence state in $x = 2$ composition.

The resistivity measurements [$\rho(T)$] show that there is small increase in normal state resistivity of $x = 1$ than $x = 0$, whereas appreciable increase in $x = 2$ composition (Fig. 6). Generally, the increase in ionic radii at rare-earth (*RE*) site causes increase in normal state resistivity in isovalent substitutions [5,27]. But here isovalent substitution in spacer layers shows some anomaly, i.e. resistivity is increasing with decreasing ionic radii. We found that, the structural changes are causing decrease in Cu valence state in $x = 2$ composition. In the cuprates, since CuO_2 planes contribute in charge transport, the decrease in Cu valence may be the reason for decrease in carriers. This decrease in carriers is thus, causing increase in normal state resistivity. A hump in resistivity measurement is also observed near 140 K in all composition. The sharpness of hump is increasing with increasing x. Luo et al. [26] studied Co-1212 ($CoSr_2Y_{1-x}Ca_xCu_2O_7$) with doping Ca atom at Y-site up

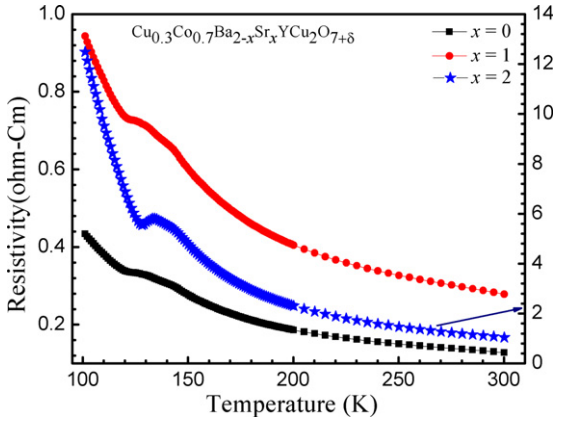

Fig. 6. Resistivity behaviour with temperature [$\rho(T)$] of $Cu_{0.3}Co_{0.7}Ba_{2-x}Sr_xYCu_2O_{7+\delta}$ ($x = 0$, 1 and 2) from 300 K to 100 K.

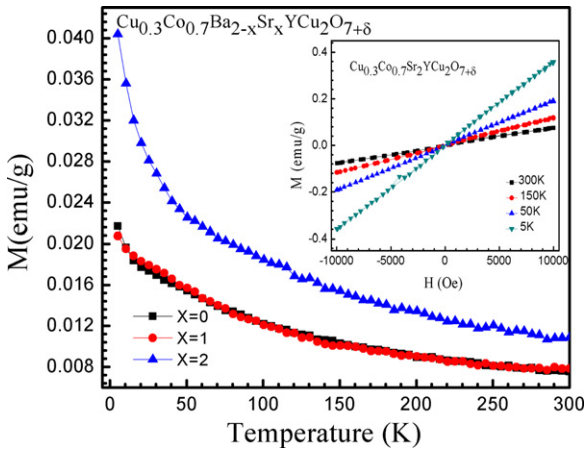

Fig. 7. ZFC magnetization behaviour with temperature [*M–T*] of $Cu_{0.3}Co_{0.7}Ba_{2-x}Sr_xYCu_2O_{7+\delta}$ ($x = 0$, 1 and 2) samples from 300 K to 5 K in applied field of 0.1 T. Inset shows *M–H* curves of the $x = 2$ sample at 5 K, 50 K, 150 K and 300 K up to magnetic field 1 T.

to $x = 40\%$. They observed similar kinds of behaviour in $x = 20\%$ to 40% composition around 145 K and explained with participation of holes in Cu/CoO_x chains/planes, in charge transport. Since, an increase in Co valence state is observed in our XPS analysis with increasing x. The observed hump in $\rho(T)$ behaviour may be due to these induced holes in Cu/CoO_x chains/planes which are taking part in charge transport and causing a dip in resistivity. These holes entered in Cu/CoO_x chains, also destruct the effective antiferromagnetic coupling [26]. But here it seems the $Cu_{0.3}Co_{0.7}$ ratio in chains is responsible for destruction of the effective antiferromagnetic coupling, since all compositions have almost similar magnetic behaviour. The magnetization with temperature (*M–T* measurement) performed in applied magnetic field $H = 0.1$ T shows paramagnetic nature of the studied samples (Fig. 7). Inset of Fig. 7 shows *M–H* curve of the $x = 2$ sample at 5 K, 50 K, 150 K and 300 K up to applied magnetic field 1 T. The *M–H* loops also indicate about paramagnetic nature of the samples. The paramagnetic nature and its magnitude is almost same for $x = 0$ and 1 composition but it has increased for $x = 2$ composition. The Co-1212 ($CoSr_2YCu_2O_7$) phase shows some antiferromagnetic ordering [8,24,28] near 150 K which was thought to originate by Co^{3+} spin [28]. An ordering of antiferromagnetic to ferromagnetic is observed in $Co_{1-x}Fe_xSr_2YCu_2O_7$ with increasing Fe content [24]. The intermediate compositions of that series were ordered in paramagnetic nature. The competition of antiferromagnetic nature of Co ions and ferromagnetic nature of Fe ions resulted in paramagnetic ordering of intermediate compositions. But here the presence of Cu ions prevents Co ions to order antiferromagnetically and leads to paramagnetic nature of the studied compounds.

4. Conclusions

With increasing Sr concentration decrease in lattice parameters is observed. The calculated tolerance factor of the systems is in accord with lattice parameter changes. This shows Sr ions replaces Ba ions in the studied samples successfully and results in electronic pressure change. The XPS measurement shows that Cu is in mixed 1+/2+ state and its valence state slightly decreases with increasing x, whereas Co is in mixed 3+/4+ state and with increasing x its valence state increases. The changes observed in electronic structure are due to structural changes in unit cell crystallization. The resistivity measurements indicate that holes in Cu/CoO_x planes taking part in charge transport. The observed magnetic behaviour of studied samples is due to the presence Cu ions in Cu/CoO_x chains/planes.

Acknowledgements

The authors would like to thank DNPL Prof. R.C. Budhani for his constant support and encouragement. One of the authors Shiva Kumar would like to acknowledge *CSIR*, India for providing fellowships.

References

[1] R. Gagnon, C. Lupien, L. Taillefer, Phys. Rev. B 50 (1994) 3458.
[2] P.C.W. Fung, W.Y. Knok, J. Supercond. 4 (1991) 415.
[3] N. Nucker, E. Pellegrin, P. Schweiss, J. Fink, S.L. Molodtsov, C.T. Simons, G. Kaindl, W. Frentrup, A. Erb, G. Muller Vogt, Phys. Rev. B 51 (1995) 8529.
[4] H. Oesterreicher, J. Alloys Compd. 335 (2002) 95.
[5] Y. Xu, S.S. Ata-Allah, M.G. Berger, O. Gluck, Phys. Rev. B 55 (1996) 15245.
[6] R.D. Shannon, Acta Crystallogr. Sect. A: Cryst. Phys. Diffr. Theor. Gen. Crystallogr. A32 (1976) 751.
[7] P. Berastegui, S.G. Eriksson, L.G. Johansson, J. Alloys Compd. 252 (1997) 76.
[8] S. Kumar, A. Dogra, M. Husain, H. Kishan, V.P.S. Awana, J. Alloys Compd. 352 (2010) 493.
[9] E. Kandyel, Physica C 415 (2004) 1.
[10] T. Mochiku, Y. Mihara, Y. Hata, S. Kamisawa, M. Furuyama, J. Suzuki, K. Kadowaki, N. Metoki, H. Fujii, K. Hirata, J. Phys. Soc. Jpn. 71 (2002) 790.
[11] J. Ramirez-Castellanos, Y. Matsui, E. Takayama-Muromachi, M. Isobe, J. Solid State Chem. 123 (1996) 378.
[12] J. Ramirez-Castellanos, Y. Matsui, M. Isobe, E. Takayama-Muromachi, J. Solid State Chem. 133 (1997) 434.
[13] T. Nagai, V.P.S. Awana, E. Takayama-Muromachi, A. Yamazaki, M. Karppinen, H. Yamauchi, S.K. Malik, W.B. Yelon, Y. Matsuia, J. Solid State Chem. 176 (2003) 213.
[14] P. Zolliker, D.E. Cox, J.M. Tranquada, G. Shirane, Phys. Rev. B 38 (1988) 6575.
[15] N.A. Khan, M. Mumtaz, A. Ullah, N. Hassan, A.A. Khurram, J. Alloys Compd. 507 (2010) 142.
[16] J.M. Tarascon, P. Barbaux, P.F. Mieceli, L.H. Greene, G.W. Hull, M. Eibschutz, S.A. Sunshine, Phys. Rev. B 37 (1988) 7458.
[17] D.D. Sharma, K. Sreedhar, P. Ganguly, C.N.R. Rao, Phys. Rev. B 36 (1987) 2371.
[18] D.D. Sharma, C.N.R. Rao, Solid State Commun. 65 (1988) 47.
[19] D.H. Kim, D.D. Berkley, A.M. Goldman, R.K. Schulze, M.L. Mecartney, Phys. Rev. B 37 (1988) 9745.
[20] J.B. Goodnough, J.M. Lango, L.B. Tabellem, New Series, vol. III/4a, Springer, Berlin, 1970.
[21] J. Ghijsen, L.H. Tjeng, J. van Elp, H. Eskes, J. Westerink, G.A. Sawatzky, M.T. Czyzyk, Phys. Rev. B 38 (1988) 11322.
[22] K. Hirokawa, F. Honda, M. Oku, J. Electron. Spectrosc. 6 (1975) 333.
[23] T.H. Fleisch, G.J. Mains, Appl. Surf. Sci. 10 (1982) 51.
[24] S.K. Singh, P. Kumar, M. Husain, H. Kishan, V.P.S. Awana, J. Appl. Phys. 107 (2010) 063905.
[25] J.C. Dupin, D. Gonbeau, H. Benqlilou-Moudden, Ph. Vinatier, A. Levasseur, Thin Solid Films 384 (2001) 2332.
[26] X.G. Luo, X.H. Chen, X. Liu, R.T. Wang, Y.M. Xiong, C.H. Wang, G.Y. Wang, X.G. Qiu, Phys. Rev. B 70 (2004) 054520.
[27] A. Tsukada, Y. Krockenberger, M. Noda, H. Yamamoto, D. Manske, L. Alff, M. Naito, Solid State Commun. 133 (2005) 27.
[28] V.P.S. Awana, S.K. Malik, W.B. Yelon, M. Karppinen, H. Yamauchi, Physica C 378 (2002) 155.